Physica B: Condensed Matter 533 (2018) 1–4

Contents lists available at ScienceDirect

Physica B: Condensed Matter

journal homepage: www.elsevier.com/locate/physb

Photoelectrochemical processes in organic semiconductor: Ambipolar perylene diimide thin film

Jung Yong Kim [a,b,*], In Jae Chung [a]

[a] Department of Chemical and Biomolecular Engineering, Korea Advanced Institute of Science and Technology, 291 Daehac-ro, Yuseong-gu, Daejeon, 305-701, Republic of Korea
[b] School of Chemical Engineering, Jimma Institute of Technology, Jimma University, P.O.Box 378, Jimma, Ethiopia

ARTICLE INFO

Keywords:
Photoelectrochemical cell
Organic semiconductor
Perylene diimide
Ambipolar

ABSTRACT

A thin film of *N,N′*-dioctadecyl-3,4,9,10-perylene tetracarboxylic diimide (PTCDI-C_{18}) is spin-coated on indium tin oxide (ITO) glass. Using the PTCDI-C_{18}/ITO electrode, we fabricate a photoelectrochemical cell with the ITO/PTCDI-C_{18}/Redox Electrolyte/Pt configuration. The electrochemical properties of this device are investigated as a function of hydroquinone (HQ) concentration, bias voltage, and wavelength of light. Anodic photocurrent is observed at $V \geq -0.2$ V vs. Ag/AgCl, indicating that the PTCDI-C_{18} film acts as an n-type semiconductor as usual. However, when benzoquinone (BQ) is inserted into the electrolyte system instead of HQ, cathodic photocurrent is observed at $V \leq 0.0$ V, displaying that PTCDI-C_{18} abnormally serves as a p-type semiconductor. Hence the overall results reveal that the PTCDI-C_{18} film can be an ambipolar functional semiconductor depending on the redox couple in the appropriate voltage.

1. Introduction

Organic semiconductors (OSCs) containing a conjugated π-electron system can transport charges and be used as functional electronic materials in plastic solar cells, flexible displays, sensors, and low-cost printed electronic circuits [1–6]. When these OSC molecules form solids, each molecule is bonded together by a weak van der Waals force, which allows for the electronic wave functions to be partially delocalized and the material to have a low dielectric constant [1,2]. These characteristics are directly related with the optical and electrical properties of OSCs, in which the charge transport behavior is generally described as hopping process rather than band conduction [4–7]. To date, significant research has been carried out to improve these relatively lower charge mobilities and efficiencies in organic devices [8–10]. However, if there is a suitable solubilizing moiety in the molecular framework, such as an alkyl chain, the weak intermolecular interactions afford some advantages such as low-temperature solution processibility [11]. Processibility is essential for realizing a key long-term vision for organic electronics: inexpensive mass production of organic devices using a large area roll-to-roll process [11–13].

OSC's two major classes are small molecules and conjugated polymers, which are further categorized as hole- and electron-transporting materials, also called p- and n-types, respectively [1,2,4,6]. The type of OSC, without any intentional doping, is mainly determined by its molecular orbital energy levels. For example, if the OSC has a high electron affinity, i.e., electron deficient state, it usually serves as an n-channel material in a transistor [3,14]. This distinction in OSCs is different from that in conventional inorganic semiconductors (ISCs). In ISCs such as Si, Ge, and GaAs, dopant molecules (acceptor: B, In, Al; donor: P, As, Sb) are introduced into an intrinsic ISC to fabricate an n- or p-type ISC with a target resistivity of $\sim 10^{5}$-$10^{-2}\,\Omega\,\mathrm{cm}$ [15]. OSCs are known to be unintentionally doped, which leads to the free carrier densities of 10^{11}-10^{15} and 10^{15}-$10^{17}\,\mathrm{cm}^{-3}$ for small molecules and polymers, respectively [16].

Perylene tetracarboxylic diimide (PTCDI) derivatives are one of several promising n-type OSCs, along with fullerene, naphthalene diimides, and several oligothiophene derivatives, because of their high electron mobilities, excellent stability, and other optoelectronic properties [17–24]. These materials have been utilized in various electronic devices such as solar cells and transistors [25,26]. In this study, we employ the solution-processed PTCDI-C_{18} thin film for another application, the photoelectrochemical cell (PECC) [27–30]. Here, we pay special attention to both the direction and magnitude of current flow [31,32]. If anodic photocurrent (i.e., the oxidation of a redox couple in an

---

[*] Corresponding author. Department of Chemical and Biomolecular Engineering, Korea Advanced Institute of Science and Technology, 291 Daehac-ro, Yuseong-gu, Daejeon, 305-701, Republic of Korea.
E-mail address: jykim@kaist.ac.kr (J.Y. Kim).

https://doi.org/10.1016/j.physb.2017.12.063
Received 12 October 2017; Received in revised form 19 December 2017; Accepted 26 December 2017
Available online 27 December 2017
0921-4526/© 2017 Elsevier B.V. All rights reserved.

electrolyte solution under light) flows, it indicates that the PTCDI-C_{18} film acts as an n-type semiconductor [33].

2. Experimental

The PECC has the ITO/PTCDI-C_{18}/Electrolyte(0.1 M tetrabutylammonium hexafluorophosphate ($TBAPF_6$) in acetonitrile)/Pt (Ag/AgCl) configuration, in which ITO/PTCDI-C_{18}, Pt, and Ag/AgCl serve as working, counter, and reference electrodes (*WE*, *CE*, and *RE*), respectively (Fig. 1a). The PTCDI-C_{18} film was spin-coated on ITO glass from a solution in chloroform (15–20 mg/mL) at 1000 rpm for several seconds and then at 2000 rpm for 30 s. The film was 150–200 nm thick, which was measured by atomic force microscope (AFM). After coating the film dried in vacuum at 25 °C for several hours. Using this film, we fabricated a PECC in a glove box under nitrogen. The cell performance was examined under illumination of monochromatic light ($\lambda = 537$ nm) with intensity of 1.3 mW/cm^2 or white light with intensity of 100 mW/cm^2.

3. Results and discussion

Fig. 1b shows the chemical structure of PTCDI-C_{18}, which was synthesized by the condensation reaction of 3,4,9,10-perylene tetracarboxylic dianhydride with octadecylamine [34]. This chemical is quite soluble and spin-coatable due to its long alkyl groups. AFM and optical microscope images of a film are shown in Fig. 1c and d, respectively, displaying an oblong-shape crystal with size of about 250 nm × 1 μm.

Cyclic voltammetry was carried out to study the electrochemical behavior of the PTCDI-C_{18} and the redox couples, hydroquinone (HQ) and benzoquinone (BQ). Fig. 2 shows cyclic voltammograms (CVs) of PTCDI-C_{18}, and its inset displays the CVs of HQ and BQ. HQ reveals oxidation (E_{ox}) and reduction potentials (E_{red}) at 0.80 and −0.28 V, respectively, which were determined at the onset point. The E_{red} of BQ is the same as HQ, but, in BQ, E_{ox} is not observed. These CV data can be converted into the energy unit (eV) vs. vacuum energy level, based on the empirical relation: $E_{LUMO/HOMO} = -E_{red/ox} - 4.4$ [35]. The highest occupied molecular orbital (HOMO = −5.20 eV) and the lowest unoccupied molecular orbital (LUMO = −4.12 eV) of HQ were thus obtained (Table 1). For PTCDI-C_{18}, E_{red} is −0.35 V in the film state and −0.62 V in solution. The smaller E_{red} of the film material than that of solution is from the π-stacking properties of the crystalline PTCDI-C_{18} film. Furthermore, by subtracting the optical bandgap, we obtained HOMO energy levels of −6.12 eV for the film and −6.04 eV for the solution, respectively (Table 2).

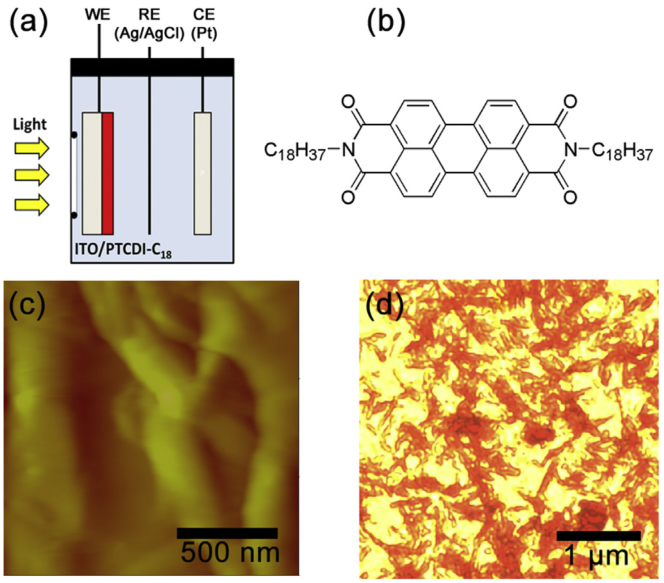

Fig. 1. (a) A photoelectrochemical cell. (b) Chemical structure of PTCDI-C_{18}. (c) AFM image of spin-coated PTCDI-C_{18} film under tapping mode, and (d) optical microscope image of spin-coated PTCDI-C_{18} film.

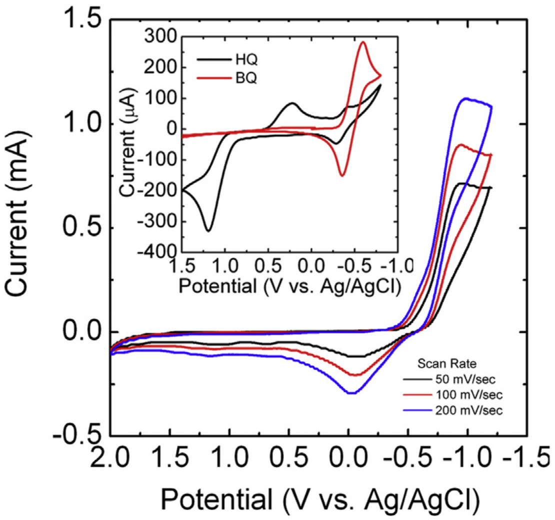

Fig. 2. CV for the spin-coated PTCDI-C_{18} film on ITO *WE* in 0.1 M $TBAPF_6$/acetonitrile with Ag/AgCl *RE* and platinum *CE* at scan rate of 50–200 mV/s. Inset: CVs for 20 mM of HQ or BQ in 0.1 M $TBAPF_6$/acetonitrile with platinum *WE*, Ag/AgCl *RE* and platinum *CE* at scan rate of 100 mV/s.

Table 1
LUMO and HOMO of HQ and BQ based on the onset potential.

	E_{red} (V)[a]	LUMO (eV)	E_{ox}[a]	HOMO (eV)
HQ	−0.27	−4.12	0.80	−5.2
BQ	−0.27	−4.13	–	–

[a] V vs. Ag/AgCl.

Fig. 3a shows the PECC photocurrent generation as a function of HQ concentration. The photocurrent increases dramatically up to 10 mM and then is saturated. This behavior indicates that, when the concentration is less than 10 mM, the mass transfer of HQ to the electrode surface is a limiting factor for the electrode reaction. However, when the concentration is more than 10 mM, charge transfer at the electrode surface becomes the major limiting factor.

Fig. 3b displays the action spectrum of the PTCDI-C_{18}–based PECC with 20 mM HQ in electrolyte solution, which resembles the normalized ultraviolet visible (UV–Vis) absorption spectrum of the film, confirming that PTCDI-C_{18} is actively working to generate free charge carriers under light. However, the incident photon to current efficiency (IPCE) is very small, indicating that, in the PECC, recombination of photo-generated charges is significant. One reason should be from the limited area at the ITO/PTCDI-C_{18}/Electrolyte interface. In solar cells containing a single OSC, it is known that exciton separation takes place at OSC/metal interfaces and is quite inefficient [36]. Moving this separation process into the organic film with an organic donor/acceptor combination and increasing surface area is the reason why the bulk heterojunction has come to be the benchmark design for high efficiency organic photovoltaics [13,37].

Table 2
E_{red}, LUMO, HOMO, and optical bandgap (E_g) of PTCDI-C_{18}. Under the same conditions, ferrocene shows E_{ox} at 0.40 V vs. Ag/AgCl, which corresponds to HOMO of −4.8 eV.

	E_{red} (V)[a]	LUMO (eV)	HOMO (eV)[b]	E_g (eV)
Solution	−0.62	−3.78	−6.04	2.26
Film	−0.35	−4.05	−6.12	2.07

[a] V vs. Ag/AgCl.
[b] HOMO = LUMO - E_g.

Download English Version:

https://daneshyari.com/en/article/8161294

Download Persian Version:

https://daneshyari.com/article/8161294

Daneshyari.com